A New Automatic Parameter Setting Method of a Simplified PCNN for Image Segmentation

Yuli Chen, Sung-Kee Park, Yide Ma, and Rajeshkanna Ala

***Abstract*— An automatic parameter setting method of a simplified pulse coupled neural network (SPCNN) is proposed here. Our method successfully determines all the adjustable parameters in SPCNN and does not need any training and trials as required by previous methods. In order to achieve this goal, we try to derive the general formulae of dynamic threshold and internal activity of the SPCNN according to the dynamic properties of neurons, and then deduce the sub-intensity range expression of each segment based on the general formulae. Besides, we extract information from an input image, such as the standard deviation and the optimal histogram threshold of the image, and attempt to build a direct relation between the dynamic properties of neurons and the static properties of each input image. Finally, the experimental segmentation results of the gray natural images from the Berkeley Segmentation Dataset, rather than synthetic images, prove the validity and efficiency of our proposed automatic parameter setting method of SPCNN.**

***Index Terms*— Automatic parameter setting, dynamic property, general formulae, image segmentation, optimal histogram threshold, simplified pulse coupled neural network, standard deviation, static property, sub-intensity range.**

I. Introduction

ECHORN'S cortical model, a bio-inspired neural network, was developed in light of synchronous dynamics of neuronal activity in cat visual cortex [1]–[3]. According to its ability to cause the adjacent neurons with similar inputs to pulse synchronously, it was soon recognized as having significant potential in image processing. Therefore, pulse coupled neural network (PCNN) model, a tailored and modified version of Echorn's cortical model, was developed by Johnson *et al*. and became more suitable for image processing [4]–[10]. Nowadays the standard PCNN model is usually simplified to achieve lower computational complexity while remaining the essential visual cortical property. The representative simplified models include the intersecting cortical model [11]–[13], the unit-linking PCNN model [14], [15] and the spiking cortical model (SCM) [16].

The past decade has seen the rapid development of PCNN in many aspects within the image processing field, such as image segmentation [7], [17]–[24], image shadow removal [25], image understanding [26], feature extraction [5], [14], [27], [28], pattern recognition [29], [30] and object recognition [31]–[33]. More detailed applications of PCNN can be found from literatures of Lindblad and Kinser [13], Ma [34] and Wang [35].

Among the applications in image processing, PCNN has great potential for developing image segmentation algorithm. However, the quality of the segmentation results strongly depends on the appropriate values of PCNN parameters. Moreover, the appropriate values of the parameters could only be adjusted manually or estimated through a heavy training, which has become a serious problem and constrained the further development of PCNN.

Many researchers have attempted to solve this problem. For example, Kuntimad and Ranganath [17] determined the minimum amplitude value of dynamic threshold which guarantees each neuron fires exactly once during a pulsing cycle, and analyzed the minimum and maximum values of linking strength β for a perfect image segmentation after acquiring the intensity ranges of object and background. Based on this principle of linking strength β, Karvonen [18] computed a specific value of the linking strength β according to the distribution information of the segments obtained from training synthetic aperture radar images. Stewart *et al*. [19] proposed a region growing PCNN for multi-value image segmentation, but it requires to manually set the time-variant dynamic threshold E and linking strength β with incremental constants. The method introduced by Bi *et al*. [24] determined the weight matrixes and linking strength β adaptively according to spatial and gray characteristics, but they empirically set the amplitude and decrement constant of dynamic threshold E. In addition, Yonekawa *et al*. [23] automatically adjusted the linking strength β, synaptic weight W and exponential decay coefficient α_e but it required many iterations of trials.

So far, most of the previous methods could not set all the parameters of PCNN automatically, except the methods proposed by Berg *et al*. [21] and Ma *et al*. [22]. The former is to evolve PCNN neurons by automatic design of algorithms through evolution, while the latter is to build an automated PCNN system based on genetic algorithm [22]. However, these algorithms require repetition of trials and a heavy

Manuscript received March 20, 2010; revised March 2, 2011; accepted March 6, 2011. Date of publication May 5, 2011; date of current version June 2, 2011. This work was supported in part by the National Science Foundation of China under Grant 60872109 and the Korea Institute of Science and Technology.

Y. Chen is with the School of Information Science and Engineering, Lanzhou University, Lanzhou, Gansu 730000, China. She is also with the Center for Cognitive Robotics Research, Robotics/Systems Division, Korea Institute of Science and Technology, Seoul 136-791, Korea (Corresponding author e-mail: chenyuli2008@live.cn).

S.-K. Park and R. Ala are with the Center for Cognitive Robotics Research, Robotics/Systems Division, Korea Institute of Science and Technology, Seoul 136-791, Korea (e-mail: skee@kist.re.kr; ala_rajeshkanna@yahoo.co.in).

Y. Ma is with the School of Information Science and Engineering, Lanzhou University, Gansu 730000, China (e-mail: ydma@lzu.edu.cn).

Color versions of one or more of the figures in this paper are available online at http://ieeexplore.ieee.org.

Digital Object Identifier 10.1109/TNN.2011.2128880

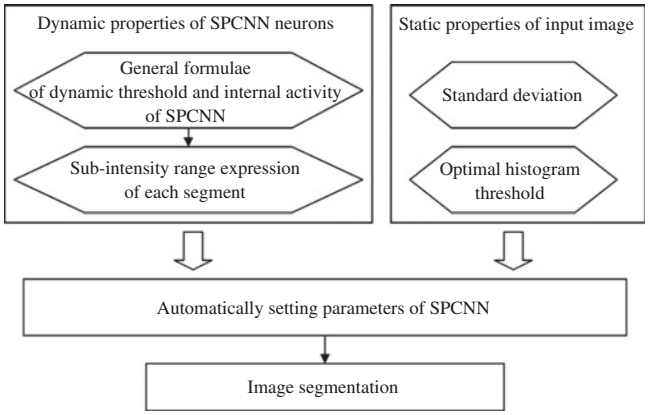

Fig. 1. General flow chart of the proposed method.

training before obtaining the proper values of parameters, which costs a lot of run time and also may not be feasible in practice.

Here, we propose a new automatic parameter setting method for the simplified PCNN (SPCNN) based on SCM [16]. In this method, we attempt to build a direct relation between the dynamic properties of neurons and the static properties of each input image, and use it to determine the proper parameter values. The proposed method does not involve any prior training and trials, which can be quite suitable for real-time image processing. A general flow chart of the proposed method is shown in Fig. 1.

The following part of this paper is divided into six sections. Section II gives a brief description of the PCNN models including a basic PCNN model and the SPCNN model, and shows the capture behavior of neurons. Section III mainly focuses on the derivation of the general formulae of dynamic threshold E_{ij} and internal activity U_{ij} of the SPCNN model. Section IV derives the sub-intensity range expression of each segment based on the general formulae. Section V elucidates the role of each parameter of SPCNN and proposes our automatic parameter setting method based on Sections III and IV. Section VI shows the experimental estimated values of the SPCNN parameters for several natural gray images of the Berkeley Segmentation Dataset, and evaluates the segmentation results. In the last section, a conclusion is made and some issues for further research are suggested.

II. PCNN Models and Capture Behavior

A. Basic PCNN Model

PCNN differs from the general artificial neural networks in having only a single layer formed by a 2-D array of laterally linked pulse coupled neurons and not requiring any training [4]–[10], [17]. The relation between image pixels and the network neurons is a one-to-one correspondence [17].

The basic PCNN was elaborated by Ranganath and Kuntimad [7] and the discrete model was described by Lindblad and Kinser [13] as follows:

$$F_{ij}[n] = e^{-\alpha_f} F_{ij}[n-1] + V_F \sum_{kl} M_{ijkl} Y_{kl}[n-1] + S_{ij} \tag{1}$$

$$L_{ij}[n] = e^{-\alpha_l} L_{ij}[n-1] + V_L \sum_{kl} W_{ijkl} Y_{kl}[n-1] \tag{2}$$

$$U_{ij}[n] = F_{ij}[n](1 + \beta L_{ij}[n]) \tag{3}$$

$$Y_{ij}[n] = \begin{cases} 1, & \text{if } U_{ij}[n] > E_{ij}[n-1] \\ 0, & \text{else} \end{cases} \tag{4}$$

$$E_{ij}[n] = e^{-\alpha_e} E_{ij}[n-1] + V_E Y_{ij}[n]. \tag{5}$$

Neuron N_{ij} in the position (i, j) has two main inputs in iteration n: feeding input $F_{ij}[n]$ and linking input $L_{ij}[n]$, which associate with neighboring neurons through constant synaptic weights M and W, respectively, and retain the previous input states by exponential decay factors $e^{-\alpha_f}$ and $e^{-\alpha_l}$, respectively. Additionally, the feeding input F_{ij} receives an input stimulus S_{ij} (a normalized gray intensity). These two inputs are then modulated through linking strength β to yield internal activity $U_{ij}[n]$ which is compared with the dynamic threshold $E_{ij}[n-1]$ of the previous iteration to judge whether neuron N_{ij} fires ($Y_{ij}[n] = 1$) or not ($Y_{ij}[n] = 0$). Subsequently, if neuron N_{ij} fires, the dynamic threshold would increase by amplitude V_E suddenly, if neuron N_{ij} does not fire, the dynamic threshold would decay by a factor $e^{-\alpha_e}$. In addition, $Y_{kl}[n-1]$ denotes the output of neighboring neuron N_{kl} in the previous iteration. The parameters V_F, V_L and V_E denote the amplitudes of feeding input F, linking input L and dynamic threshold E, respectively. And the parameters α_f, α_l, α_e denote the exponential decay coefficients of F, L and E, respectively [13].

B. SPCNN Model

Nowadays there have been a number of modified models of PCNN. It has been proved that the SCM has lower computational complexity and high accuracy rates when compared with other methods such as Gabor, PCNN, etc. [16]. Therefore, a SPCNN model derived from Zhan *et al*'s. SCM model [16] is employed in our work and described as follows:

$$U_{ij}[n] = e^{-\alpha_f} U_{ij}[n-1] + S_{ij}\left(1 + \beta V_L \sum_{kl} W_{ijkl} Y_{kl}[n-1]\right) \tag{6}$$

$$Y_{ij}[n] = \begin{cases} 1, & \text{if} \quad U_{ij}[n] > E_{ij}[n-1] \\ 0, & \text{else} \end{cases} \tag{7}$$

$$E_{ij}[n] = e^{-\alpha_e} E_{ij}[n-1] + V_E Y_{ij}[n] \tag{8}$$

where all the notations have the same meaning as indicated in (1)–(5). The only difference between this SPCNN and the SCM lies in the firing condition, in this model, the traditional firing condition $U_{ij}[n] > E_{ij}[n-1]$ rather than the sigmoid function used in [16] is adopted, since it is the most widely applied firing condition and there is no difference between them in determining neurons firing.

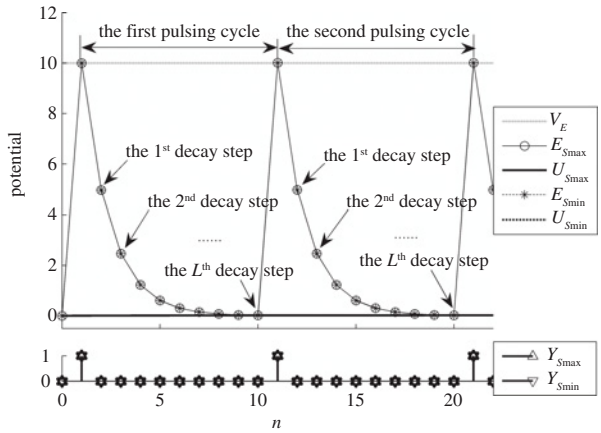

Fig. 2. Synchronous periodic activity of two neurons with the same minimum non-zero gray intensity $S = 0.0039 \approx 1/225$ in a two-neuron SPCNN model which uses manually set parameter values $\alpha_f = 0.2$, $\beta = 0.1$, $V_L = 1$, $\alpha_e = 0.7$, and $V_E = 10$. Each fire period of the neurons is referred as "a pulsing cycle" and the decay steps within each pulsing cycle are illustrated.

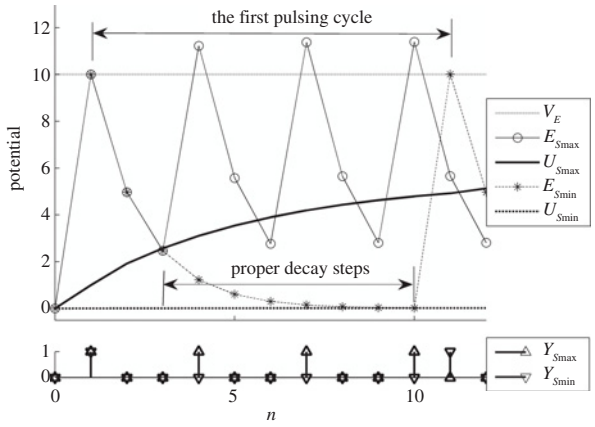

Fig. 3. Activity of two neurons with the maximum intensity $S_{\max} = 1$ and the minimum nonzero intensity $S_{\min} = 0.0039$, respectively, in a two-neuron SPCNN model which uses the same manually set parameter values as in Fig. 2. Obviously, the neuron with the maximum intensity fires more frequently than the one with the minimum nonzero intensity. Within the first pulsing cycle, the "proper decay steps" after which the neurons are able to produce pulses are marked.

According to [16], the internal activity $U_{ij}[n]$ has two terms $U_{ij}[n] = U_1 + U_2$. The first term $U_1 = (\exp(-\alpha_f))U_{ij}[n-1]$ records the previous neuron state by an exponential decay factor. The second term is the result of the modulation of a simplified linking input

$$L_{ij}[n] = V_L \sum_{kl} W_{ijkl} Y_{kl}[n-1] \tag{9}$$

and a simplified feeding input

$$F_{ij}[n] = S_{ij} \tag{10}$$

in a nonlinear fashion [17]

$$\begin{aligned} U_2 &= F_{ij}[n](1 + \beta L_{ij}[n]) \\ &= S_{ij}\left(1 + \beta V_L \sum_{kl} W_{ijkl} Y_{kl}[n-1]\right). \end{aligned} \tag{11}$$

There are totally five adjustable parameters in the SPCNN model: α_f, β, V_L, V_E, and α_e. How to automatically set proper values to these parameters will be explained in Section V. In this paper, we also deal with a two-neuron SPCNN model which is only for illustrating the properties of the full-linking model.

C. Capture Behavior

As is well known, the neurons with higher intensity stimuli always fire prior to the ones with lower intensity stimuli in PCNN-based models, i.e., their fire periods satisfy

$$T_{high} < T_{low}. \tag{12}$$

Consequently, the minimum intensity neuron has the longest fire period T_{lowest}, which is referred as "a pulsing cycle" [17]. The "pulsing cycles" and the decay steps within each pulsing cycle (each decay step corresponds to an iteration of the neural model) are shown in Fig. 2, where the synchronous activity of two neurons with the same minimum nonzero intensity $S = 0.0039 \approx 1/255$ in a two-neuron SPCNN model is illustrated.

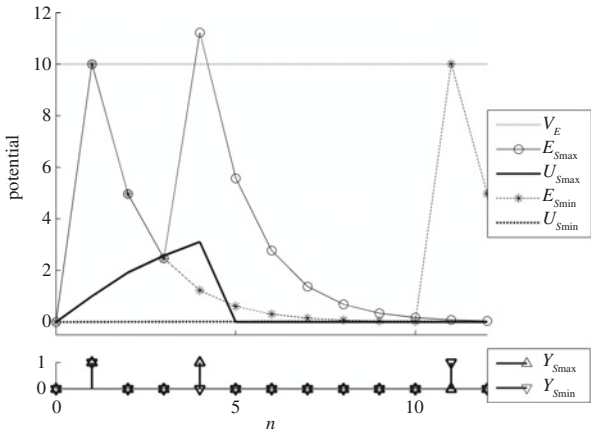

Fig. 4. Way to prevent the neuron which has fired twice from firing again is to set the internal activity $U_{S\max}$ of the neuron to zero in the subsequent iterations. The internal activity $S_{\max} = 1$ of the neuron with the maximum intensity in a two-neuron SPCNN model is illustrated as an example. This model uses the same manually set parameter values as in Fig. 2 (another neuron with intensity $S_{\min} = 0.0039$).

Since $T_{high} < T_{low}$, higher intensity neurons fire more frequently than the lower ones as shown in Fig. 3, the pulses produced by higher intensity neurons and those by lower ones would mix together when

$$T_{low} = pT_{high}, \qquad p = 2, 3, \ldots \tag{13}$$

This phenomenon indicates that any single pixel with relatively high intensity may be grouped into two or more segments, which goes against the purpose of image segmentation. To avoid such case, we assume that any neuron in the SPCNN could fire once and only once after the first common fire. In this paper, once a neuron fires twice, it would be prevented from firing again by setting its internal activity U_{ij} to zero as shown in Fig. 4. In the end, the SPCNN process is stopped after the minimum nonzero intensity neurons fire for the second time which denotes the end of the first pulsing cycle. Therefore, it is significant to study the dynamic properties of

neurons within the first pulsing cycle in the SPCNN. Within the first pulsing cycle, the decay steps after which the neurons are able to produce pulses are referred as "proper decay steps." The "proper decay steps" in a two-neuron SPCNN model are shown in Fig. 3 as an example.

III. General Formulae of Dynamic Threshold E and Internal Activity U

In order to fully understand the dynamic properties of SPCNN neurons and unveil the relationship between the dynamic properties and the SPCNN parameters, the general formulae of dynamic threshold E_{ij} and internal activity U_{ij} of neuron N_{ij} could be carefully studied. We firstly analyze the general formulae in the full-linking SPCNN model, and then deduce the general formulae in a two-neuron SPCNN model as a particular case.

A. General Formulae in the Full-Linking SPCNN Model

When the full-linking SPCNN model illustrated in (6)–(8) is applied to process images, the synaptic weight is a matrix

$$W_{ijkl} = \begin{bmatrix} 0.5 & 1 & 0.5 \\ 1 & 0 & 1 \\ 0.5 & 1 & 0.5 \end{bmatrix}. \tag{14}$$

According to (6), the value of the term $\sum_{kl} W_{ijkl} Y_{kl}[n-1]$ varies with different combinations of the eight previous neighboring outputs. All the nonzero intensity neurons with initial states of $U[0] = 0$, $Y[0] = 0$, and $E[0] = 0$ would fire in the first iteration $Y[1] = 1$ (the first firing time could be recorded as $n_1 = 1$) because the firing condition $U[1] = S > E[0]$ is always satisfied. Therefore, supposing that all the image pixels are nonzero, then the term $\sum_{kl} W_{ijkl} Y_{kl}[1] = 6$ is a constant in the internal activity formula in the second iteration

$$U_{ij}[2] = U_{ij}[n_1 + 1] = S_{ij}(e^{-\alpha_f} + 1 + 6\beta V_L) = S_{ij} M[2] \tag{15}$$

where notation $M[n]$ is used to represent the factor multiplied by neuron intensity in the internal activity formula in the nth iteration ($M[1] = 1$).

And according to (8), the dynamic threshold increases by amplitude V_E in the first iteration when all the neurons fire

$$E_{ij}[1] = E_{ij}[n_1] = V_E. \tag{16}$$

It is noted that in order to inhibit all the neurons in the second iteration, i.e., $Y[2] = 0$, the value of the amplitude V_E should not be less than that of the internal activity of the maximum intensity neuron in the second iteration, i.e., no neuron can satisfy the firing condition $U_{S\max}[2] \le E_{ij}[1] = V_E$. Otherwise, some neurons would fire in the second iteration and the number of the fired neurons only depends on the value of the amplitude V_E. Therefore, the corresponding fired pixels would form an image segment regardless of the property of the input image, which would impede the image segmentation performance.

Subsequently, since $Y[2] = 0$ the dynamic threshold decreases by $e^{-\alpha_e}$ in the second iteration and the term $\sum_{kl} W_{ijkl} Y_{kl}[2] = 0$ is eliminated from the internal activity formula in the third iteration

$$E_{ij}[2] = E_{ij}[n_1 + 1] = V_E e^{-\alpha_e} \tag{17}$$

$$\begin{aligned} U_{ij}[3] &= U_{ij}[n_1 + 1 + 1] \\ &= e^{-\alpha_f} U_{ij}[2] + S_{ij}\left(1 + \beta V_L \sum_{kl} W_{ijkl} Y_{kl}[2]\right) \\ &= S_{ij}(e^{-\alpha_f} M[2] + 1) = S_{ij}\left(\frac{1 - e^{-3\alpha_f}}{1 - e^{-\alpha_f}} + 6\beta V_L e^{-\alpha_f}\right) \\ &= S_{ij} M[3]. \end{aligned} \tag{18}$$

In the following iterations, the internal activity U_{ij} becomes more complex, since it depends on not only the previous internal activity but also on the specific combination of the previous neighboring outputs which vary spatially and temporally. Even so, there is still a general formula with recursion form for the internal activity U_{ij}.

According to the SPCNN model (6)–(8), the dynamic threshold E_{ij} in the decay step l and the internal activity U_{ij} in the decay step $l + 1$ within the first pulsing cycle could be written as

$$E_{ij}[n_1 + l] = V_E e^{-l\alpha_e} \tag{19}$$

$$\begin{aligned} U_{ij}[n_1 + l + 1] &= e^{-\alpha_f} U_{ij}[n_1 + l] \\ &\quad + S_{ij}\left(1 + \beta V_L \sum_{kl} W_{ijkl} Y_{kl}[n_1 + l]\right) \\ &= S_{ij}\left(e^{-\alpha_f} M[n_1 + l] + 1 + \beta V_L \sum_{kl} W_{ijkl} Y_{kl}[n_1 + l]\right) \\ &= S_{ij} M[n_1 + l + 1]. \end{aligned} \tag{20}$$

The neurons that satisfy the firing condition

$$U_{ij}[n_1 + l + 1] > E_{ij}[n_1 + l] \tag{21}$$

would fire synchronously in the decay step $l + 1$

$$Y_{ij}[n_1 + l + 1] = 1. \tag{22}$$

And the dynamic threshold would increase to

$$E_{ij}[n_1 + l + 1] = V_E(e^{-(l+1)\alpha_e} + 1) \tag{23}$$

and then keep attenuating. It is noted that once a neuron fires, it would be prevented from firing again by setting its internal activity U_{ij} to zero in the subsequent iterations as mentioned previously.

B. General Formulae in a Two-N SPCNN Model

A two-neuron SPCNN model as a particular case of the full-linking model could be obtained by simplifying the synaptic weight to $W_{ijkl} = 1$, then the internal activity in (6) becomes

$$U_i[n] = e^{-\alpha_f} U_i[n-1] + S_i(1 + \beta V_L Y_k[n-1]). \tag{24}$$

It is possible to deduce the exact general formulae of dynamic threshold E_i and internal activity U_i in any decay step of any pulsing cycle in a two-neuron SPCNN (see appendix for the complete detail derivation). Here, we focus on the first pulsing cycle. The general formulae of dynamic threshold

E_i and internal activity U_i within the first pulsing cycle are concluded as

$$E_i[n_1 + l] = V_E e^{-l\alpha_e} \tag{25}$$

$$U_i[n_1 + l + 1] = S_i \left(\frac{1 - e^{-(n_1+l+1)\alpha_f}}{1 - e^{-\alpha_f}} + \beta V_L e^{-l\alpha_f} \right) = S_i \tilde{M}[n_1 + l + 1] \tag{26}$$

where $n_1 = 1$ denotes the first common firing time of neurons, and the notation $\tilde{M}[n]$ is used to distinguish from the notation $M[n]$ in the full-linking SPCNN model.

IV. Sub-Intensity Range of Each Segment

As discussed in Section III, the SPCNN neurons that satisfy the firing condition (21) would fire synchronously in the decay step $l + 1$ within the first pulsing cycle ($n_1 = 1$) and the corresponding pixels would form an image segment. Therefore, the whole image can be divided into several segments. The following part will discuss the sub-intensity range of a segment captured in a proper decay step.

According to (12), higher intensity neurons always fire prior to the lower ones. Therefore, the sub-intensity range of the neurons firing in the decay step $l+1$ could be interpreted as the range from the higher critical intensity whose corresponding neurons cannot satisfy the firing condition in the decay step l to the lower critical intensity whose corresponding neurons can still satisfy the firing condition in the decay step $l + 1$

$$\begin{cases} U_{S_{\text{high}}}[1 + l] \le E[1 + l - 1] \\ U_{S_{\text{low}}}[1 + l + 1] > E[1 + l]. \end{cases} \tag{27}$$

According to (20), the above conditions are rewritten as

$$\begin{cases} S_{\text{high}} \cdot M[1 + l] \le E[1 + l - 1] \\ S_{\text{low}} \cdot M[1 + l + 1] > E[1 + l]. \end{cases} \tag{28}$$

Then the sub-intensity range S of the segment captured in the decay step $l + 1$ could be derived as

$$S_{\text{high}} = \frac{E[1 + l - 1]}{M[1 + l]} \ge S > \frac{E[1 + l]}{M[1 + l + 1]} = S_{\text{low}}. \tag{29}$$

Since each sub-intensity range S ranges between [1, 0] and should have more than one intensity pixel to form a segment, the above sub-intensity range could be further described as

$$\min(1, S_{\text{high}}) \ge S \ge \max(0, S_{\text{low}}), \Delta S > \frac{1}{225}. \tag{30}$$

It is noted that the exact sub-intensity range of each image segment can only be determined while the real image segmentation process is run by the full-linking SPCNN. This is because the general formula of the internal activity U_{ij} in (20) is a recursion formula and the value of the internal activity depends on the specific combination of neighboring outputs. Whereas, the sub-intensity ranges in a two-neuron SPCNN can be exactly calculated since the internal activity U_i in (26) is a determined function of iteration time. Therefore, for a simple preview of the segmentation process of the full-linking SPCNN, we demonstrate how to obtain the exact sub-intensity ranges in a two-neuron SPCNN in the following.

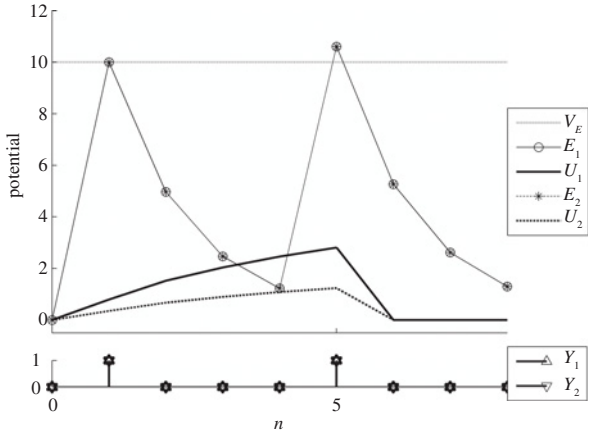

Fig. 5. Synchronous activity of two neurons with intensities $S_1 = 0.79216$ and $S_2 = 0.34902$, respectively, in a two-neuron SPCNN model which uses the same manually set parameter values as in Fig. 2. These two intensities are the boundary values of the sub-intensity range $0.79216 \ge S \ge 0.34902$ in the $l + 1 = 4$ decay step ($n = n_1 + l + 1 = 5$).

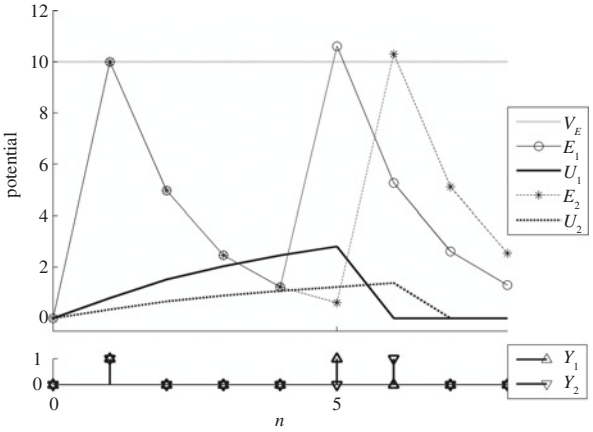

Fig. 6. Asynchronous activity of two neurons with intensities $S_1 = 0.79216$ and $S_2 = 0.3451$ (the intensity next to $S = 0.34902$), respectively, in the same two-neuron SPCNN model as in Fig. 5. This occurrence of asynchrony reflects the accuracy of the calculation of the sub-intensity range $0.79612 \ge S \ge 0.34902$ in the $l + 1 = 4$ decay step.

A. Sub-Intensity Ranges in a Two-Neuron SPCNN Model

Given a set of parameter values for the two-neuron SPCNN, it is possible to calculate each sub-intensity range exactly. For example, given the parameters $\alpha_f = 0.2$, $\beta = 0.1$, $V_L = 1$, $\alpha_e = 0.7$ and $V_E = 10$, the calculation of numerical sub-intensity range in the decay step $l + 1 = 4$ is demonstrated. According to (27), the neurons that fire in the decay step $l + 1 = 4$ (i.e., $n = n_1 + l + 1 = 5$) as shown in Fig. 5 satisfies the conditions

$$\begin{cases} U[4] \le E[3] \\ U[5] > E[4] \end{cases} \tag{31}$$

and then according to (29) and (30) the sub-intensity range can be written as

$$\min\left(1, \frac{E[3]}{\tilde{M}[4]}\right) \ge S \ge \max\left(0, \frac{E[4]}{\tilde{M}[5]}\right), \quad \Delta S > \frac{1}{255}. \tag{32}$$

Furthermore, plug the general formulae of dynamic threshold and internal activity of the two-neuron SPCNN (25) and

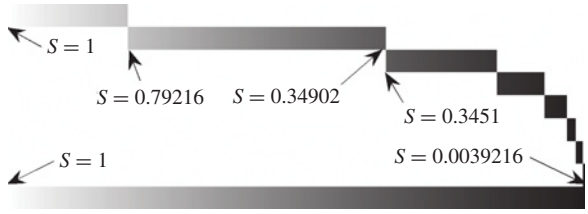

Fig. 7. Sub-intensity range in each proper decay step within the first pulsing cycle in a two-neuron SPCNN model is shown in each upper row. The last row is the overall intensity range which combines all the sub-intensity ranges. This model uses the same manually set parameter values as in Fig. 2.

TABLE I
NUMERICAL INTENSITY RANGES CAPTURED IN EACH PROPER DECAY STEP WITHIN THE FIRST PULSING CYCLE

Decay Step $l+1$	Intensity Range S
3rd	1–0.79608
4th	0.79216–0.34902
5th	0.3451–0.15686
6th	0.15294–0.07451
7th	0.070588–0.035294
8th	0.031373–0.019608
9th	0.015686–0.0078431
10th	0.0039216–0.0039216

(26) into (32), the resulting numerical sub-intensity range is $0.79216 \geq S \geq 0.34902$ as shown in the second row of Fig. 7. In addition, the accuracy of the sub-intensity range can be tested by reducing the lower limit to the next intensity $S = 0.3451$ and checking whether the pulses of the two neurons are still keeping synchronous. As seen from Fig. 6, the asynchrony of pulses occurs immediately, which proves that the resulting sub-intensity range $0.79216 \geq S \geq 0.34902$ is accurate, and the derivation process of the general formulae is also correct.

Similarly, other sub-intensity ranges can be calculated and the results have been listed in Table I. Finally, by combining all the sub-intensity ranges within the first pulsing cycle, an overall intensity range covering the range $1 \geq S \geq 0.0039216$ can be obtained and shown in the bottom row of Fig. 7.

V. AUTOMATIC PARAMETER SETTING METHOD OF SPCNN

There are totally five adjustable parameters in the SPCNN model—α_f, β, V_L, V_E, and α_e. Each of them plays a special role in the neural behaviors. For the purpose of assigning proper values to these SPCNN parameters, a hierarchical segmentation strategy is adopted to segment a natural image consisting of more than two scenes/objects. In other words, an input image is firstly divided into two coarse regions. The region with higher intensities is output as the first segment region, whereas the other region with lower intensities is further segmented into several finer regions in the following SPCNN iterations. This is consistent with the intuition that different scenes/objects in a gray image are usually depicted with different degrees of darkness. In this paper, we attempt

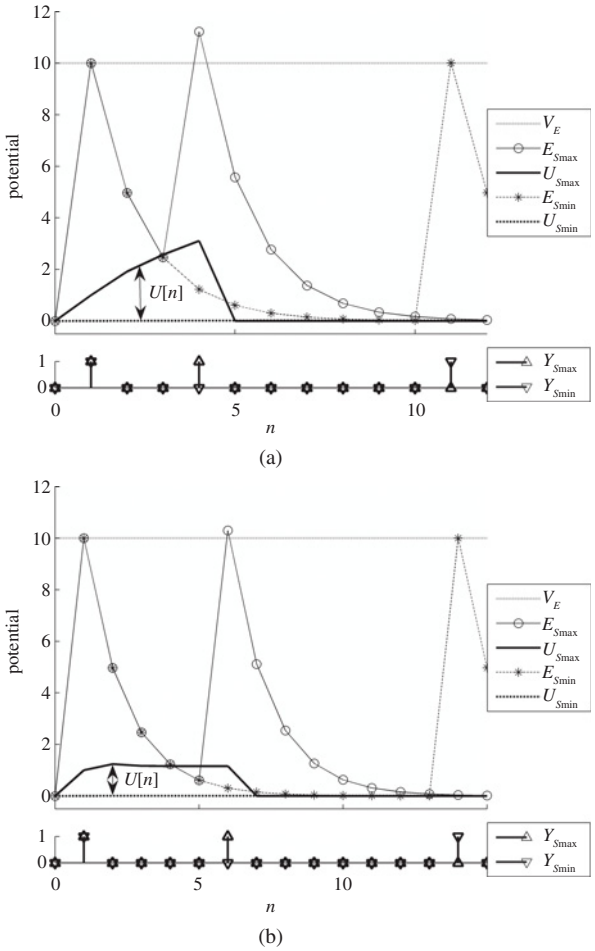

Fig. 8. Distribution range of internal activity $U[n]$ varies with different values of parameter $\alpha_f[\alpha_f = 0.2$ in graph (a) and $\alpha_f = 2$ in graph (b)] in a two-neuron SPCNN model whose other parameter values are same as in Fig. 2. The distribution range of means the range between the internal activities $U_{S\max}[n]$ and $U_{S\min}[n]$ (where $S_{\max} = 1$ and $S_{\min} = 0.0039$). Obviously, the smaller the value of α_f, the wider the distribution range of $U[n]$ becomes. Therefore, the value of α_f has a certain inverse relation to the standard deviation of the normalized image intensities.

to build a direct relation between the dynamic behaviors of SPCNN neurons and the static properties of each image segmented under this hierarchical strategy. Consequently based on this relation, a novel automatic parameter setting method has been developed. And the way to set each parameter is elucidated as follows.

A. Parameter α_f

The parameter α_f is the exponential decay coefficient of internal activity. The value of parameter α_f affects the distribution range of internal activity $U[n]$. The distribution range of $U[n]$ means the range between $U_{S\max}[n]$ and $U_{S\min}[n]$ which corresponds to the boundary normalized intensities $S_{\max} = 1$ and $S_{\min} = 0.0039$ as shown in Fig. 8. The only difference between the two graphs of Fig. 8 lies in the value of the parameter α_f: graph (a) with $\alpha_f = 0.2$ and graph (b) with $\alpha_f = 2$. Obviously, the lower the value of α_f, the wider the distribution range of internal activity $U[n]$ becomes, which indicates that there is a certain inverse relation between the

TABLE II
PARAMETERS OF SPCNN AUTOMATICALLY ESTIMATED FOR EACH IMAGE (WITH A FIX V_L)

	V_L (fix)	β	α_f	V_E	α_e
Exp. 1	1	0.0721	1.4724	1.6620	0.5445
Exp. 2		0.1458	1.3864	2.1250	0.9563
Exp. 3		0.1040	1.4312	1.8632	0.7390
Exp. 4		0.1264	1.0444	2.1105	0.7560
Exp. 5		0.3646	1.9518	3.3295	1.9749
Exp. 6		0.1093	1.2436	1.9442	0.7241
Exp. 7		0.2670	1.7495	2.7759	1.5835
Exp. 8		0.4405	1.6003	3.8447	2.0651
Exp. 9		0.1761	1.5404	2.2707	1.1446

TABLE III
PARAMETERS OF SPCNN AUTOMATICALLY ESTIMATED FOR EACH IMAGE (WITH A RANDOM V_L)

	V_L (random)	β	α_f	V_E	α_e
Exp. 1	0.3529	0.2043	1.4724	1.6620	0.5445
Exp. 2	0.9501	0.1535	1.3864	2.1250	0.9563
Exp. 3	0.4447	0.2339	1.4312	1.8632	0.7390
Exp. 4	0.6154	0.2054	1.0444	2.1105	0.7560
Exp. 5	0.1389	2.6250	1.9518	3.3295	1.9749
Exp. 6	0.0579	1.8881	1.2436	1.9442	0.7241
Exp. 7	0.8132	0.3284	1.7495	2.7759	1.5835
Exp. 8	0.2028	2.1723	1.6003	3.8447	2.0651
Exp. 9	0.3816	0.4615	1.5404	2.2707	1.1446

value of parameter α_f and the standard deviation σ of the input image I with normalized intensities. Through a large number of experiments, we found that the logarithmic function of the reciprocal of the image standard deviation σ could be suitable for the description of this relation. Therefore, the value of parameter α_f could be calculated as

$$\alpha_f = \log\left(\frac{1}{\sigma(I)}\right). \tag{33}$$

It is noted that the standard deviation σ of the normalized intensities is always less than 1, so the value of α_f is always larger than zero, which prevents the $U_{ij}[n]$ in (6) from growing exponentially with the increase of n and guarantees the physical meaning of the internal activity.

B. Parameter β

The parameter β is the linking strength among neurons. Based on the given V_L, the larger the value of β, the more strongly a neuron is affected by its neighboring neurons, which leads to a more drastic fluctuation in internal activity $U_{ij}[n]$.

The range of β for possible perfect image segmentation of a two-region image has been deduced by Kuntimad and Ranganath [17] as follows:

$$\beta_{\max} = \frac{(S_{R\max}/S_{B\max}) - 1}{L_{B\max}} \tag{34}$$

$$\beta_{\min} = \max\left[\frac{(S_{R\max}/S_{R\min}) - 1}{L_{R\min}}, \frac{(S_{B\max}/S_{B\min}) - 1}{L_{B\min}}\right] \tag{35}$$

where $S_{R\max}$ and $S_{B\max}$ denote the maximum gray intensities of the higher intensity region and the lower intensity region, respectively; $S_{R\min}$ and $S_{B\min}$ denote the minimum gray intensities of the higher intensity region and the lower intensity region, respectively; $L_{R\min}$ represents the minimum value of the linking inputs that $S_{R\min}$ receives from the firing pixels in the higher intensity region; $L_{B\min}$ represents the minimum value of the linking inputs that $S_{B\min}$ receives from the firing pixels in the lower intensity region; and $L_{B\max}$ is the maximum value of the linking inputs that $S_{B\max}$ receives from the firing pixels in the higher intensity region (see [17] for details).

To roughly separate the two coarse regions of an input image at the initial stage of our hierarchical strategy, we need to select a proper value for the parameter β. Here, we could resort to (34) and (35) which are the possible conditions of parameter β for PCNN to segment a two-region image perfectly. The perfect segmentation, however, is guaranteed only if $\beta_{\min}$ happens to be less than $\beta_{\max}$ (note that $\beta_{\min}$ may be larger than $\beta_{\max}$), which depends on the values of $L_{R\min}$, $L_{B\min}$ and $L_{B\max}$, and the extent of the overlap of the two intensity ranges [17]. Therefore, a perfect segmentation, which means capturing each region separately in its entirety, may not always be possible for a complex natural image [17]. Generally speaking, it may be impossible to assign precise values to the parameters of PCNN-based models for an exactly perfect segmentation. In such a case, it is feasible to select an approximate value for the parameters to achieve a reasonable segmentation instead of a perfect segmentation. Our task at the initial stage is to separate the image into two coarse regions other than to segment it perfectly, which suits the above case well. Therefore, we would choose the value $\beta_{\max}$ in (34) as the approximate value for parameter β

$$\beta = \beta_{\max}. \tag{36}$$

The reason to choose $\beta_{\max}$ rather than the $\beta_{\min}$ in (35) is because its value could be calculated without knowing prior the values of $L_{R\min}$, $L_{B\min}$ and the extent of the intensity overlap which are often unknown for a new image. The key to compute the $\beta_{\max}$ in (34) is to calculate the maximum intensity of the coarse region with lower intensities, i.e., $S_{B\max}$. Since the value $S_{B\max}$ varies with different images, it is necessary to build a bridge to connect the $S_{B\max}$ and a specific image. We found that the bridge could be directly established by specifying the image optimal histogram threshold to the $S_{B\max}$. In this paper, the optimal histogram threshold S' is determined by Otsu's method. Because Otsu's method is characterized by its nonparametric and unsupervised nature of threshold selection, and it can automatically choose an optimal threshold to minimize the within-class variance and maximize the between-class variance [36]. This is a desired characteristic for us to reasonably separate an image into two coarse regions. Therefore

$$S_{B\max} = S'. \tag{37}$$

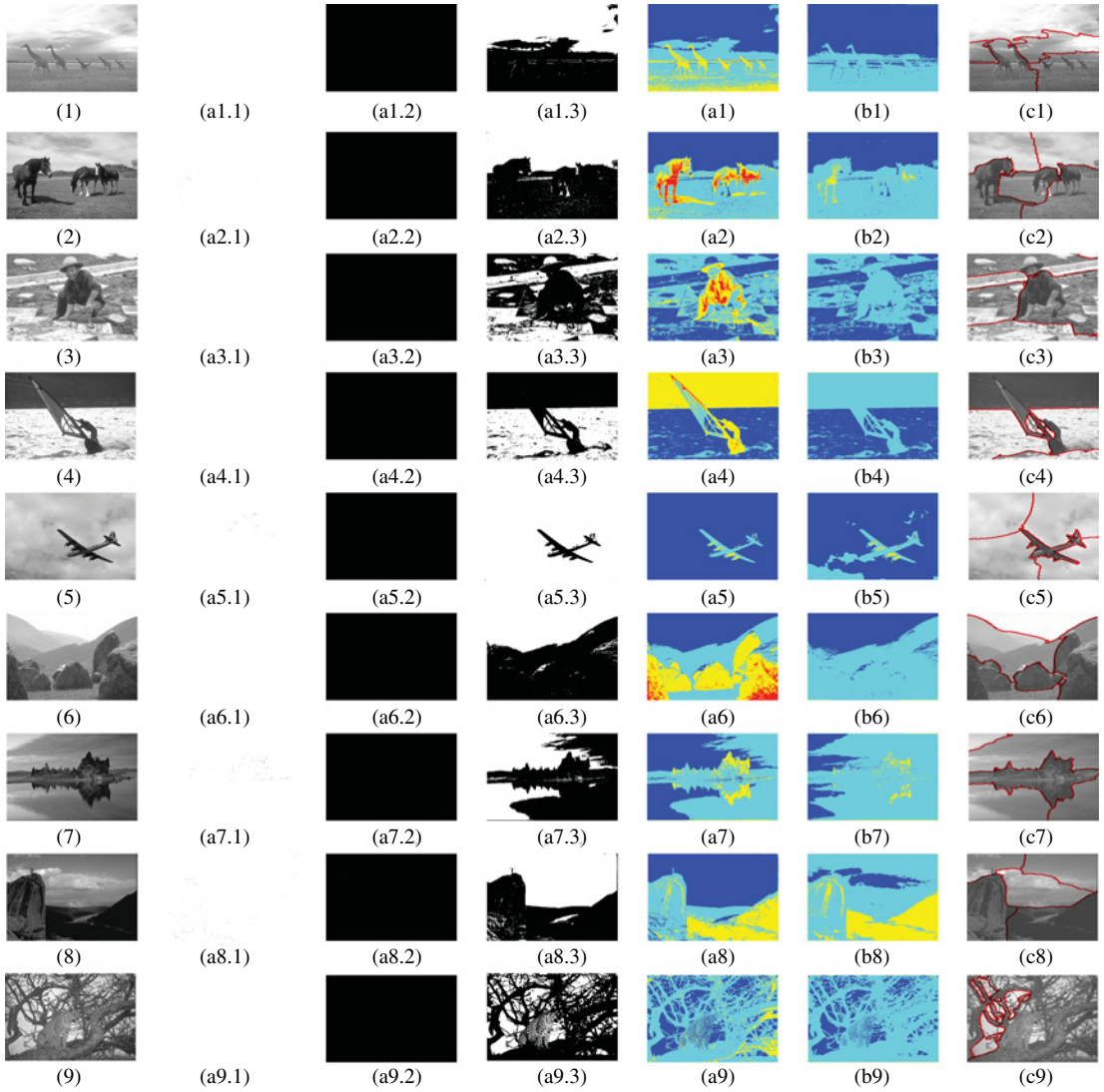

Fig. 9. Segmentation results of nine natural gray images from the Berkeley Segmentation Dataset. Each row illustrates the experiment of one image. Images in the first column are the original input images. Images in columns (a.1), (a.2) and (a.3) are the output pulsing images processed by the SPCNN in iteration times $n = 1, 2$, and 3, respectively, images in column (a) are the final segmentation results processed by the SPCNN with the proposed automatic parameter setting method. Images in column (b) are the segmentation results of a basic PCNN with a set of commonly used empirical parameter values ($\alpha_l = 1.0$, $\alpha_e = 0.1$, $\alpha_f = 0.1$, $V_F = 0.5$, $V_L = 0.2$, and $V_E = 20$) [38]. Images in column (c) are the segmentation results processed by the normalized cuts method [39]. For images (1)–(8), the segmentation results in columns (a) have better performance than the ones in columns (b) and (c), since they are much better at separating the main scenes/objects in the original images into meaningful regions with more natural shape. For image (9), all the segmentation results (a9), (b9) and (c9) are ineffective due to the low contrast among the scenes/objects in the image. (Image resolution: 300 dpi for gray images and 400 dpi for color images.)

Besides, the maximum intensity of image, i.e., $S_{\max}$ could be assigned to $S_{R\max}$

$$S_{R\max} = S_{\max} \tag{38}$$

and the possible maximum value of the linking input $L = 6V_L$ obtained according to (9) and (14) could be assigned to $L_{B\max}$

$$L_{B\max} = 6V_L. \tag{39}$$

Finally, the value of parameter β could be calculated by substituting (37)–(39) into (34)

$$\beta = \frac{(S_{\max}/S') - 1}{6V_L}. \tag{40}$$

C. Parameter V_L

The parameter V_L is the amplitude of linking input L. Actually, V_L can be any random positive value, and the value of β correspondingly changes according to (40). Because the term βV_L always acts as a factor as a whole in the SPCNN, the specific value of V_L does not affect the final result of segmentation (Tables II, III and Fig. 9). Here, we could fix

$$V_L = 1. \tag{41}$$

D. Parameter α_e

The parameter α_e is the exponential decay coefficient of dynamic threshold E and is significant to image segmentation

precision. The larger the value of α_e, the lower the segmentation precision is (i.e., a larger sub-intensity range is captured in a proper decay step, especially in the initial proper decay steps). The way to set α_e will be explained later along with the setting of V_E.

E. Parameter V_E

The parameter V_E is the amplitude of dynamic threshold E. The values of V_E and α_e could be deduced from the expression of the first sub-intensity range S when assuming that the first image segment is captured in the decay step $l+1=2$ (i.e., $n=n_1+l+1=3$). Then, according to (29), the first sub-intensity range could be expressed as

$$\frac{E[1]}{M[2]} \geq S \geq \frac{E[2]}{M[3]}. \tag{42}$$

As mentioned previously, the coarse region with higher intensities is output as the first image segment, so the first sub-intensity range would range from the maximum image intensity "1" to the maximum intensity of the coarse region with lower intensities, that is, $1 \geq S > S_{B\max}$. According to (37), $S_{B\max} = S'$. Therefore, the first sub-intensity range is $1 \geq S > S'$ and thus it could be rewritten as

$$\frac{E[1]}{M[2]} \geq 1 \geq S > S' \geq \frac{E[2]}{M[3]}. \tag{43}$$

Finally, substitute (16) and (17) into (43), and thus parameters V_E and α_e could be derived as follows:

$$\frac{E[1]}{M[2]} \geq 1 \rightarrow \frac{V_E}{M[2]} \geq 1 \rightarrow V_E \geq M[2] \tag{44}$$

$$\frac{E[2]}{M[3]} \leq S' \rightarrow \frac{V_E e^{-\alpha_e}}{M[3]} \leq S' \rightarrow \alpha_e \geq \ln \frac{V_E}{S' M[3]} \tag{45}$$

where

$$M[2] = e^{-\alpha_f} + 1 + 6\beta V_L \tag{46}$$

and

$$M[3] = \frac{1-e^{-3\alpha_f}}{1-e^{-\alpha_f}} + 6\beta V_L e^{-\alpha_f} \tag{47}$$

which are derived from (15) and (18), respectively.

In order to obtain a unique value for each of the parameters V_E and α_e, the lower limits are adopted

$$V_E = M[2] \tag{48}$$

and

$$\alpha_e = \ln \frac{V_E}{S' M[3]}. \tag{49}$$

In summary, the automatically set values of the SPCNN parameters could be seen as the results of the interaction between the dynamic properties of neurons and the static properties of a specific image (such as the standard deviation and the optimal histogram threshold). Besides, the SPCNN parameters are not completely independent but interact with each other.

VI. Experiments and Analysis

In this section, several natural gray images from the Berkeley Segmentation Dataset [37], rather than synthetic images used in [17] and [21], are used as experimental images. The experiments are run on MATLAB 7.0 with Intel Core 2 Duo E8500 3.17 GHz PC.

For each experimental image, the values of the five adjustable SPCNN parameters could be estimated by the proposed automatic parameter setting method, i.e., (33), (40), (41), (48), and (49) in Section V. The resulting parameter values are shown in each row of Table II (with fixed V_L) and Table III (with random V_L). With these estimated parameter values, the SPCNN would perform image segmentation for each input image.

In order to terminate the SPCNN process properly, a ratio R is computed in each of the iterations after $n=3$

$$R = \frac{Num_{\text{fired}}}{Num_{\text{all}}} \tag{50}$$

where Num_{fired} denotes the number of the fired neurons in the current iteration and Num_{all} denotes the total number of neurons. If the value of the ratio R is larger than a small positive number ε, i.e., $R > \varepsilon$ (here, $\varepsilon = (1/25)^2 = 0.0016$), it indicates that the segmented region in the current iteration is meaningful. Otherwise, it implies that the fired neurons in the current iteration may only correspond to some scattered pixels or a meaningless region, and thus, the SPCNN process is terminated and all the left unfired pixels are grouped into the previous segment. It is noted that a large ε may prevent the appearance of some meaningful regions, while a too small ε probably allows the meaningless segments to appear. Here, we adopt the value $\varepsilon = (1/25)^2 = 0.0016$ after plenty of tests, assuming that the area of a meaningful region should be larger than ε times of that of the whole image.

Alternatively, the SPCNN process could also be terminated earlier in the iteration when the number of the unfired pixels is equal to the number of the zero pixels of the image. This is because the zero pixels will never fire in the whole SPCNN process.

Both of the parameter values in Tables II and III lead to the same image segmentation results as shown in column (a) of Fig. 9. The average processing time for each image in our experiment is about 1 s.

In addition, a comparison of segmentation performance is conducted among three different methods to evaluate the validity of the proposed automatic parameter setting method of SPCNN. Two other common segmentation methods are employed. One is the basic PCNN with a set of commonly used empirical parameter values ($\alpha_l = 1.0$, $\alpha_e = 1.0$, $\alpha_f = 0.1$, $V_F = 0.5$, $V_L = 0.2$, $V_E = 20$, and $\beta = 0.1$) [38] and the other one is the normalized cuts method proposed by Shi and Malik [39] (code available on Jianbo Shi's webpage).

The SPCNN segmentation process and the comparison results are shown in Fig. 9. Images in the first column of Fig. 9 are the original natural gray images. Images from the second column to the fifth column are the output images of the SPCNN with the proposed automatic parameter setting method. Among them, the fully white images (except the

pixels with intensity "0") in column (a.1) indicate the common fire of neurons in the first iteration $n = 1$; and the fully black images in column (a.2) indicate the common inhibition of neurons in the second iteration $n = 2$; moreover, each image in column (a.3) contains two areas (i.e., white and black) which represent the two initial coarse regions segmented in the third iteration $n = 3$. And the white area is outputted as the first segment of the image; whereas the black area is further separated into several finer segments in the following SPCNN iterations. In the end, the final image segmentation results of the SPCNN are shown in column (a) with different colors to indicate different scenes/objects in the images. For comparison, images in column (b) are the contrast segmentation results processed by the basic PCNN with a set of commonly used empirical parameter values [38]. And images in column (c) are the contrast segmentation results obtained by the normalized cuts method which treats image segmentation as a hierarchical graph partitioning problem based on a perceptual grouping [39].

In order to verify the validity of the proposed automatic parameter setting method of SPCNN, we demonstrate how the resulting estimated values of the parameters vary with the specific input images. For this purpose, we select the parameters β and α_e as representatives. As discussed in Section V, when given the value of V_L, the larger the value of β, the more strongly a neuron would be influenced by its neighbors. This means a bigger area of neighboring pixels would be captured to form a segment. Besides, the larger the value of α_e, the lower the segmentation precision would be. This means a larger sub-intensity range of segment would exist in each of the initial SPCNN iterations. As seen from Table II, both the minimum values of parameters β and α_e occurred in Exp. 1 when given $V_L = 1$, which indicates that the image would be segmented with a higher precision. This is in accordance with the elaborate property of the first input image. On the contrary, both the maximum values of parameters β and α_e appeared in Exp. 8, which means that the image would be segmented roughly. This is also accordant with the massive property of the eighth input image. Therefore, the proposed method is capable of assigning proper values to the parameters of SPCNN in terms of different images, which is the main contribution of the proposed method.

In addition, another contribution of the proposed automatic parameter setting method of SPCNN lies in its capability of improving image segmentation performance, which can be seen from the performance comparison of segmentation results in columns (a), (b), and (c) of the first eight rows in Fig. 9. Obviously, the segmentation results in column (a) which are processed by the SPCNN are better at separating the scenes/objects in the images into meaningful regions with more natural shapes. Whereas, the results in column (b) which are obtained by the basic PCNN tend to merge some scenes/objects in the images together, because the empirically set values of the basic PCNN parameters may not be suitable for all the input images; and the results in column (c) which are performed by the normalized cuts method seem to have difficulty in effectively locating and separating the scenes/objects in the input images except the seventh one. For example, regarding the first input image in the first row, the main scenes of sky, grassland and giraffes have been well separated by the SPCNN with the proposed automatic parameter setting method as shown in (a1). In contrast, the result in (b1) could not distinguish the scenes of grassland and giraffes, and the result in (c1) gives meaningless image segments. Therefore, it is obvious that SPCNN with the proposed automatic parameter setting method is of great potential in processing image segmentation, especially to process the images with a relatively high contrast among the scenes/objects in the images. It is noted that all these segmentation methods are ineffective to locate the leopard on the tree in image (9) because of the low contrast among the scenes/objects in the image.

VII. Conclusion

In this paper, we presented an automatic parameter setting method for estimating values to all the adjustable parameters of a SCM-based [16] SPCNN model in terms of different images. Adjusting parameter values manually or by a heavy prior training [7], [17]–[24] has become a crucial problem of PCNN-based segmentation. The method proposed in this paper attempted to resolve this problem by establishing a direct relation between the dynamic properties of neurons and the static properties of an input image. The dynamic properties of neurons were analyzed in several aspects, such as the distribution range of internal activity $U[n]$, the general formulae of dynamic threshold E_{ij} and internal activity U_{ij}, and the sub-intensity range of a segment captured in each proper decay step. Meanwhile, the static properties of an input image included the standard deviation and the optimal histogram threshold of the image.

The established direct relation provided a feasible way to automatically estimate all the parameters values of SPCNN for each input image, and it did not need any training and trials. We tested the validity of the proposed automatic parameter setting method of SPCNN with several natural gray images from the Berkeley Segmentation Dataset [37]. The resulting segmentation results were compared with the ones processed by other two methods: the basic PCNN with a set of commonly used empirical parameter values [38] and the normalize cuts method proposed by Shi and Malik [39]. It can be seen that the results of the proposed method have outperformed the ones of previous methods in identifying the scenes of the images. Therefore, the proposed automatic parameter setting method of SPCNN can be an effective approach to resolve the problem of parameter estimation for the PCNN-based segmentation.

Our future work includes extracting more features from the input images, such as texture and color information, to improve the segmentation effect, and extending our research to segment images with low contrast regions.

Appendix

The general formulae of dynamic threshold $E_i[n]$ and internal activity $U_i[n]$ in the nth iteration of a two-neuron SPCNN model are deduced according to the dynamical equations of the model in (7), (8), and (24) as follows.

Here, it is supposed that the two neurons N_i and N_k have similar intensities and can be captured by each other. The initial states of the two neurons are zeros

$$U_i[0] = 0, \quad Y_i[0] = 0, \quad E_i[0] = 0$$

and

$$U_k[0] = 0, \quad Y_k[0] = 0, \quad E_k[0] = 0. \tag{51}$$

Since both of the firing conditions of neurons N_i and N_k are satisfied when $n = 1$

$$U_i[1] = S_i > E_i[0] = 0$$

and

$$U_k[1] = S_k > E_k[0] = 0 \tag{52}$$

thus, both neurons N_i and N_k produce pulses

$$Y_i[1] = 1 \text{ and } Y_k[1] = 1 \tag{53}$$

and both of their dynamic thresholds increase

$$E_i[1] = V_E \text{ and } E_k[1] = V_E \tag{54}$$

here, the first common firing time is notated as $n_1 = 1$.

In the following, only the states of neuron N_i are demonstrated since the two neurons captured by each other have the same behavior.

When $n = 2$, the internal activity of neuron N_i is

$$\begin{aligned} &U_i[2] = U_i[n_1 + 1] = e^{-\alpha_f} U_i[1] + S_i(1 + \beta V_L Y_k[1]) \\ &= S_i(e^{-\alpha_f} + 1 + \beta V_L) = S_i\left(\tfrac{1-e^{-2\alpha_f}}{1-e^{-\alpha_f}} + \beta V_L\right) = S_i \tilde{M}[2]. \end{aligned} \tag{55}$$

Since the amplitude V_E of the dynamic threshold is assumed to be large enough that the firing condition cannot be satisfied in the iteration $n = 2$

$$U_i[2] \le E_i[1] = V_E \tag{56}$$

thus, neuron N_i does not fire in $n = 2$

$$Y_i[2] = 0 \tag{57}$$

and the dynamic threshold E_i decays exponentially

$$E_i[2] = V_E e^{-\alpha_e}. \tag{58}$$

Similarly, the states of neuron N_{ij} in the decay step l within the first pulsing cycle (i.e., $n = n_1 + l$) can be written as follows:

$$\begin{aligned} U_i[n_1 + l] &= S_i\left(\frac{1 - e^{-(n_1+l)\alpha_f}}{1 - e^{-\alpha_f}} + \beta V_L e^{-(l-1)\alpha_f}\right) \\ &= S_i \tilde{M}[n_1 + l] \end{aligned} \tag{59}$$

$$Y_i[n_1 + l] = 0 \tag{60}$$

$$E_i[n_1 + l] = V_E e^{-l\alpha_e}. \tag{61}$$

Supposing that the second firing time is $n = n_2 = n_1 + L + 1$ (L is the last decay step in the first pulsing cycle, see Fig. 2), the states of neuron N_i in the previous iteration $n = n_2 - 1 = n_1 + L$ can be deduced as

$$\begin{aligned} U_i[n_2 - 1] &= U_i[n_1 + L] \\ &= S_i\left(\frac{1 - e^{-(n_1+L)\alpha_f}}{1 - e^{-\alpha_f}} + \beta V_L e^{-(L-1)\alpha_f}\right) \\ &= S_i\left(\frac{1 - e^{-(n_2-1)\alpha_f}}{1 - e^{-\alpha_f}} + \beta V_L k_1 e^{-(n_2-n_1-2)\alpha_f}\right) \\ &= S_i \tilde{M}[n_2 - 1] \end{aligned} \tag{62}$$

$$Y_i[n_2 - 1] = 0 \tag{63}$$

$$E_i[n_2 - 1] = E_i[n_1 + L] = V_E e^{-L\alpha_e} = V_E h_1 e^{-(n_2-n_1-1)\alpha_e} \tag{64}$$

where $k_1 = 1$, $h_1 = 1$.

Subsequently, the internal activity of neuron N_i in the firing time $n = n_2$

$$\begin{aligned} U_i[n_2] &= S_i\left(\frac{1 - e^{-n_2\alpha_f}}{1 - e^{-\alpha_f}} + \beta V_L k_1 e^{-(n_2-n_1-1)\alpha_f}\right) \\ &= S_i \tilde{M}[n_2] \end{aligned} \tag{65}$$

satisfies the firing condition $U_i[n_2] > E_i[n_2 - 1]$, thus both neurons N_i and N_k produce pulses in $n = n_2$

$$Y_i[n_2] = 1, \quad Y_k[n_2] = 1 \tag{66}$$

and the dynamic threshold of neuron N_i increases by the amplitude V_E

$$E_i[n_2] = V_E(h_1 e^{-(n_2-n_1)\alpha_e} + 1) = V_E h_2 \tag{67}$$

where $h_2 = h_1 e^{-(n_2-n_1)\alpha_e} + 1$.

Since $Y_k[n_2] = 1$, the states of neuron N_i in the next iteration $n = n_2 + 1$ become

$$\begin{aligned} U_i[n_2 + 1] &= S_i\left(\frac{1 - e^{-(n_2+1)\alpha_f}}{1 - e^{-\alpha_f}} + \beta V_L k_2\right) \\ &= S_i \tilde{M}[n_2 + 1] \end{aligned} \tag{68}$$

$$Y_i[n_2 + 1] = 0 \tag{69}$$

$$E_i[n_2 + 1] = V_E h_2 e^{-\alpha_e} \tag{70}$$

where $k_2 = k_1 e^{-(n_2-n_1)\alpha_f} + 1$.

In summary, the dynamic threshold and internal activity of neuron N_i around the firing time $n = n_{m+1}$ can be derived as

$$E_i[n_{m+1} - 1] = V_E h_m e^{-(n_{m+1}-n_m-1)\alpha_e} \tag{71}$$

$$\begin{aligned} U_i[n_{m+1}] &= S_i\Big(\frac{1 - e^{-n_{m+1}\alpha_f}}{1 - e^{-\alpha_f}} \\ &\qquad + \beta V_L k_m e^{-(n_{m+1}-n_m-1)\alpha_f}\Big) \\ &= S_i \tilde{M}[n_{m+1}] \end{aligned} \tag{72}$$

$$E_i[n_{m+1}] = V_E h_{m+1} \tag{73}$$

$$\begin{aligned} U_i[n_{m+1} + 1] &= S_i\left(\frac{1 - e^{-(n_{m+1}+1)\alpha_f}}{1 - e^{-\alpha_f}} + \beta V_L k_{m+1}\right) \\ &= S_i \tilde{M}[n_{m+1} + 1] \end{aligned} \tag{74}$$

where

$$h_{m+1} = h_m e^{-(n_{m+1}-n_m)\alpha_e} + 1, \qquad h_1 = 1 \tag{75}$$

and

$$k_{m+1} = k_m e^{-(n_{m+1}-n_m)\alpha_f} + 1, \quad k_1 = 1 \tag{76}$$

n_{m+1} denotes the $(m+1)$th firing time of neuron N_i, $m = 0, 1, 2, \ldots$

Finally, the general formulae of dynamic threshold and internal activity of neuron N_i in the decay step l and $l+1$, respectively, within the $(m+1)$th pulsing cycle can be concluded as

$$E_i[n_{m+1}+l] = V_E h_{m+1} e^{-l\alpha_e} \tag{77}$$

$$U_i[n_{m+1}+l+1] = S_i\left(\frac{1-e^{-(n_{m+1}+l+1)\alpha_f}}{1-e^{-\alpha_f}} + \beta V_L k_{m+1} e^{-l\alpha_f}\right) \tag{78}$$

$$= S_i \tilde{M}[n_{m+1}+l+1]. \tag{79}$$

ACKNOWLEDGMENT

The authors appreciate the Editor-in-Chief, the Associate Editor and the anonymous reviewers' justified and insightful comments for improving the quality of this paper. They would also like to thank X. Li, Chang'an University, Xi'an, China, and Y. Chen, Asian Institute of Technology, Bangkok, Thailand, for their helpful discussions and constructive suggestions.

REFERENCES

[1] R. Eckhorn, H. J. Reitboeck, M. Arndt, and P. W. Dicke, "Feature linking via synchronization among distributed assemblies: Simulations of results from cat visual cortex," *Neural Comput.*, vol. 2, no. 3, pp. 293–307, 1990.

[2] R. Eckhorn, H. J. Reitboeck, M. Arndt, and P. W. Dicke, "A neural network for feature linking via synchronous activity: Results from cat visual cortex and from simulations," in *Models of Brain Function*. Cambridge, U.K.: Cambridge Univ. Press, 1989, pp. 255–272.

[3] H. J. Reitboeck, R. Eckhorn, M. Arndt, and P. W. Dicke, "A model of feature linking via correlated neural activity," in *Synergistics of Cognition*. New York: Springer-Verlag, 1989, pp. 112–125.

[4] J. L. Johnson and D. Ritter, "Observation of periodic waves in a pulse-coupled neural network," *Opt. Lett.*, vol. 18, no. 15, pp. 1253–1255, Aug. 1993.

[5] J. L. Johnson, "Pulse-coupled neural nets: Translation, rotation, scale, distortion, and intensity signal invariance for images," *Appl. Opt.*, vol. 33, no. 26, pp. 6239–6253, Sep. 1994.

[6] J. L. Johnson, "Pulse-coupled neural networks," *Proc. SPIE Adapt. Comput.: Math., Electron., Opt. Crit. Rev.*, vol. CR55, pp. 47–76, Apr. 1994.

[7] H. S. Ranganath, G. Kuntimad, and J. L. Johnson, "Pulse coupled neural networks for image processing," in *Proc. IEEE Southeastcon*, Raleigh, NC, Mar. 1995, pp. 37–43.

[8] H. S. Ranganath and G. Kuntimad, "Iterative segmentation using pulse-coupled neural networks," *Proc. SPIE Appl. Sci. Artif. Neural Netw. II*, vol. 2760, pp. 543–554, Mar. 1996.

[9] J. L. Johnson and M. L. Padgett, "PCNN models and applications," *IEEE Trans. Neural Netw.*, vol. 10, no. 3, pp. 480–498, May 1999.

[10] J. L. Johnson, M. L. Padgett, and O. Omidvar, "Guest editorial overview of pulse coupled neural network (PCNN) special issue," *IEEE Trans. Neural Netw.*, vol. 10, no. 3, pp. 461–463, May 1999.

[11] J. M. Kinser, "Simplified pulse-coupled neural network," *Proc. SPIE Appl. Sci. Artif. Neural Netw. II*, vol. 2760, pp. 563–567, Mar. 1996.

[12] U. Ekblad, J. M. Kinser, J. Atmer, and N. Zetterlund, "The intersecting cortical model in image processing," *Nucl. Instrum. Methods Phys. Res. Sec. A: Accel., Spect., Detect. Assoc. Equip.*, vol. 525, nos. 1–2, pp. 392–396, Jun. 2004.

[13] T. Lindblad and J. M. Kinser, *Image Processing Using Pulse-Coupled Neural Networks*, 2nd ed. New York: Springer-Verlag, 2005.

[14] X. Gu, "Feature extraction using unit-linking pulse coupled neural network and its applications," *Neural Process. Lett.*, vol. 27, no. 1, pp. 25–41, Feb. 2008.

[15] X. Gu, L. Zhang, and D. Yu, "General design approach to unit-linking PCNN for image processing," in *Proc. Int. Joint Conf. Neural Netw.*, vol. 3. Jul.–Aug. 2005, pp. 1836–1841.

[16] K. Zhan, H. Zhang, and Y. Ma, "New spiking cortical model for invariant texture retrieval and image processing," *IEEE Trans. Neural Netw.*, vol. 20, no. 12, pp. 1980–1986, Dec. 2009.

[17] G. Kuntimad and H. S. Ranganath, "Perfect image segmentation using pulse coupled neural networks," *IEEE Trans. Neural Netw.*, vol. 10, no. 3, pp. 591–598, May 1999.

[18] J. A. Karvonen, "Baltic sea ice SAR segmentation and classification using modified pulse-coupled neural networks," *IEEE Trans. Geosci. Remote Sens.*, vol. 42, no. 7, pp. 1566–1574, Jul. 2004.

[19] R. D. Stewart, I. Fermin, and M. Opper, "Region growing with pulse-coupled neural networks: An alternative to seeded region growing," *IEEE Trans. Neural Netw.*, vol. 13, no. 6, pp. 1557–1662, Nov. 2002.

[20] Y. Lu, J. Miao, L. Duan, Y. Qiao, and R. Jia, "A new approach to image segmentation based on simplified region growing PCNN," *Appl. Math. Comput.*, vol. 205, no. 2, pp. 807–814, Nov. 2008.

[21] H. Berg, R. Olsson, T. Lindblad, and J. Chilo, "Automatic design of pulse coupled neurons for image segmentation," *Neurocomputing*, vol. 71, nos. 10–12, pp. 1980–1993, Jun. 2008.

[22] Y. D. Ma and C. L. Qi, "Study of automated PCNN system based on genetic algorithm," *J. Syst. Simul.*, vol. 18, no. 3, pp. 722–725, 2006.

[23] M. Yonekawa and H. Kurokawa, "An automatic parameter adjustment method of pulse coupled neural network for image segmentation," in *Proc. Artif. Neural Netw.*, Limassol, Cyprus, 2009, pp. 834–843.

[24] Y. Bi, T. Qiu, X. Li, and Y. Guo, "Automatic image segmentation based on a simplified pulse coupled neural network," in *Advances in Neural Networks*, vol. 3174, F.-L. Yin, J. Wang, and C. Guo, Eds. Berlin, Germany: Springer-Verlag, 2004, pp. 199–211.

[25] X. Gu, D. Yu, and L. Zhang, "Image shadow removal using pulse coupled neural network," *IEEE Trans. Neural Netw.*, vol. 16, no. 3, pp. 692–698, May 2005.

[26] H. S. Ranganath, G. Kuntimad, and J. L. Johnson, *A Neural Network for Image Understanding*. Oxford, U.K.: Oxford Univ. Press, 1997.

[27] J. L. Johnson, "Time signatures of images," in *Proc. IEEE Int. Conf. Neural Netw.*, vol. 2. Orlando, FL, Jul. 1994, pp. 1279–1284.

[28] J. Zhang, K. Zhan, and Y. Ma, "Rotation and scale invariant antinoise PCNN features for content-based image retrieval," *Neural Netw. World*, vol. 17, no. 2, pp. 121–132, 2007.

[29] K. Waldemark, T. Lindblad, V. Becanovic, J. L. Guillen, and P. L. Klingner, "Patterns from the sky: Satellite image analysis using pulse coupled neural networks for pre-processing, segmentation and edge detection," *Pattern Recognit. Lett.*, vol. 21, no. 3, pp. 227–237, Mar. 2000.

[30] R. C. Mureşan, "Pattern recognition using pulse-coupled neural networks and discrete Fourier transforms," *Neurocomputing*, vol. 51, pp. 487–493, Apr. 2003.

[31] J. M. Kinser and J. L. Johnson, "Object isolation," *Opt. Memor. Neural Netw.*, vol. 5, no. 3, pp. 137–145, 1996.

[32] H. S. Ranganath and G. Kuntimad, "Object detection using pulse coupled neural networks," *IEEE Trans. Neural Netw.*, vol. 10, no. 3, pp. 615–620, May 1999.

[33] B. Yu and L. Zhang, "Pulse-coupled neural networks for contour and motion matchings," *IEEE Trans. Neural Netw.*, vol. 15, no. 5, pp. 1186–1201, Sep. 2004.

[34] Y. D. Ma, K. Zhan, and Z. B. Wang, *Applications of Pulse-Coupled Neural Networks*, 1st ed. Berlin, Germany: Springer-Verlag, 2010.

[35] Z. Wang, Y. Ma, F. Cheng, and L. Yang, "Review of pulse-coupled neural networks," *Image Vis. Comput.*, vol. 28, no. 1, pp. 5–13, Jan. 2010.

[36] N. Otsu, "A threshold selection method from gray-level histograms," *IEEE Trans. Syst., Man, Cybern.*, vol. 9, no. 1, pp. 62–66, Jan. 1979.

[37] D. Martin, C. Fowlkes, D. Tal, and J. Malik, "A database of human segmented natural images and its application to evaluating segmentation algorithms and measuring ecological statistics," in *Proc. 8th Int. Conf. Comput. Vis.*, vol. 2. Vancouver, BC, Canada, Jul. 2001, pp. 416–423.

[38] Y. D. Ma, L. Liu, K. Zhan, and Y. Q. Wu, "Pulse-coupled neural networks and one-class support vector machines for geometry invariant texture retrieval," *Image Vis. Comput.*, vol. 28, no. 11, pp. 1524–1529, Nov. 2010.

[39] J. Shi and J. Malik, "Normalized cuts and image segmentation," *IEEE Trans. Pattern Anal. Mach. Intell.*, vol. 22, no. 8, pp. 888–905, Aug. 2000.

Yuli Chen received the B.S. degree in electronic information science and technology from Lanzhou University, Gansu, China, in 2005. She is currently pursuing the Ph.D. degree in radio physics at Lanzhou University, and she has been under the Ph.D. dual degree program between the School of Information Science and Engineering at Lanzhou University, and the Center for Cognitive Robotics Research, Korea Institute of Science and Technology, Seoul, Korea, since 2008.

Her current research interests include artificial neural networks, image processing, object recognition, and cognitive visual processing.

Sung-Kee Park received the B.S. and M.S. degrees in mechanical design and production engineering from Seoul National University, Seoul, Korea, in 1987 and 1989, respectively. He received the Ph.D. degree from the Korea Advanced Institute of Science and Technology, Seoul, in 2000, in the area of computer vision.

He is a principal Research Scientist for Korea Institute of Science and Technology (KIST), Seoul. He has been working with the Cognitive Robotics Center at KIST. During his period at KIST, he held a visiting position at the Robotics Institute, Carnegie Mellon University, Pittsburgh, PA, in 2005, where he did research on object recognition. His current research interests include cognitive visual processing, object recognition, visual navigation, and human-robot interaction.

Yide Ma received the B.S. and M.S. degrees in radio technology from Chengdu University of Engineering Science and Technology, Sichuan, China, in 1984 and 1988, respectively. He received the Ph.D. degree from the Department of Life Science, Lanzhou University, Gansu, China, in 2001.

He is currently a Professor in the School of Information Science and Engineering, Lanzhou University. He has published more than 50 papers in major journals and international conferences and several textbooks, including *Principle and Application of Pulse Coupled Neural Network* (Beijing: Science Press, 2006), and *Principle and Application of Microcomputer* (Beijing: Science Press, 2006). His current research interests include artificial neural networks, digital image processing, pattern recognition, digital signal processing, and computer vision.

Rajeshkanna Ala received the B.E. degree in electronics and communication engineering and the M.E. degree in communication system engineering from Madurai Kamaraj University, Madurai, India, in 2001 and 2003, respectively. He is currently pursuing the Ph.D. degree in the Center for Cognitive Robotics Research, Korea Institute of Science and Technology, Seoul, Korea, affiliated to University of Science and Technology, Daejeon, Korea.

His current research interests include cognitive visual processing and computer vision.